COMPUTATIONAL FLUID DYNAMICS OF WATER VAPOR / ZEOLITE 13X ADSORPTION

By

Evan Gildernew

Sungwoo Yang
Assistant Professor, Mechanical Engineering
(Chair)

Bradley Harris
Assistant Professor, Chemical Engineering
(Committee Member)

Michael Danquah
Associate Dean
(Committee Member)

Kidambi Sreenivas
Professor, Mechanical Engineering
(Committee Member)

COMPUTATIONAL FLUID DYNAMICS OF WATER VAPOR / ZEOLITE 13X ADSORPTION

By

Evan Gildernew

A Thesis Submitted to the Faculty of the University of
Tennessee at Chattanooga in Partial
Fulfillment of the Requirement of the Degree
of Master of Engineering

The University of Tennessee at Chattanooga
Chattanooga, Tennessee

December 2021

ABSTRACT

This work describes the development of a Finite Element Model (FEM) for use in determining adsorption system performance. The considered interactions are between Zeolite 13X and water vapor for the purposes of engineering adsorbent characteristics and harvester device characteristics. Four objectives are evaluated in the development of a predictive model. First, to understand the implementation of adsorption systems equations and the assumptions that could prevent reliable predictability. Second, to assemble, reduce, and analyze model constants and approximations that express FEM coefficient calculations. Third, to analyze factor sensitivity of model inputs by way of a 2k factorial screening to determine which inputs would benefit from future model development. Fourth, to identify potential avenues of research that would result in novel intellectual property. The main findings of the solver factor screening indicate that micro-dispersion factors and intra-crystalline gas diffusivity are the highest value characteristics in relation to water uptake.

DEDICATION

To my wife Rebecca Joy and Dr. Sungwoo Yang.

ACKNOWLEDGEMENTS

Without exception my time as an undergraduate Chemical Engineering student and as a Masters student at UTC has been marked by interactions with Faculty and Staff of the highest caliber. In many instances I have witnessed portraits of brilliance, service, and mercy beyond what would be normally expected.

This subject matter has required a grinding effort with repeated reassessment of what is needed to achieve its completion. Dr. Sungwoo Yang has never failed to support the effort, encourage proper direction, and care for me as a person. His humility, energy, and focus allowed me to achieve results that seemed far out of reach.

TABLE OF CONTENTS

LIST OF TABLES

LIST OF FIGURES

LIST OF ABBREVIATIONS

AWH	Atmospheric Water Harvester
CPDF	Chemical Potential Driving Force Model
CRG	Computational research group
DOE	Department of Energy
FAU	Faujasites
GMRES	Generalized Minimal Residual Method
IUPAC	International Union of Pure and Applied Chemistry
KSP	Kyrlov Subspace methods
LDF	Linear Driving Force Model
LTE	Local Thermal Equilibrium Model
MOFS	Metal-organic Frameworks
NLTE	Non Local Thermal Equilibrium Model
PETSc	Portable, Extensible Toolkit for Scientific Computation
PSA	Pressure swing applications
REV	Representative elementary volume
TSA	Temperatures swing applications

LIST OF SYMBOLS

α	Coefficient of liquid thermal expansion
β	Affinity coefficient of adsorbent-adsorbate pair
ΔH	Isosteric enthalpy of adsorption
ε_t	Total effective porosity
ε_{Ma}	Adsorbent macro-porosity
ε_{mi}	Adsorbent micro-porosity
Γ_{atm}	Sorbent domain exposed to atmosphere
Γ_{sink}	Domain region for heat sink
Γ_{wall}	Harvester wall domain
λ_{ads}	Thermal conductivity of adsorbed phase
λ_{eff}	Effective thermal conductivity
λ_{sor}	Thermal conductivity of sorbent
λ_{vap}	Thermal conductivity of vapor
ϕ_{sor}	Characteristic particle diameter for adsorbent

μ_v Viscosity of vapor phase

ρ_b Density of bulk adsorbent $[kg/m^3]$

ρ_c Density of adsorbent particle$[kg/m^3]$

ρ_v Density of vapor phase$[kg/m^3]$

τ Tortuosity of adsorbent

A Polanyi's adsorption potential

BET_α BET Heterogeneity Factor

Cp_{ads} Specific heat of adsorbate

Cp_{sor} Specific heat of adsorbent

Cp_{vap} Temperature dependent specific heat of vapor

D_M Macro-diffusion constant

D_{sO} Intra-molecular gas diffusivity

E_a Characteristic energy of activation

E_O Characteristic energy of adsorption

H_{vap} Enthalpy of Vaporization

K Permeability

k_c Kozeny constant for adsorbent

M Molecular weight of vapor

n_s Effective micro-pore dispersion

P Partial pressure of water vapor

P_{atm} Atmospheric pressure

P_{cr} Vapor critical pressure

P_{eq} Temperature dependent vapor pressure

P_{sat} Adsorbent saturated pressure

Q Density of adsorbed phase $[kg/m^3]$

q Adsorbed mass concentration

Q_{eq} Density of equilibrium adsorbed phase $[kg/m^3]$

R_g Universal gas Constant

T_{ads} Temperature of adsorbent

T_{cr} Vapor critical temperature of vapor

T_s Temperature of sorbent

T_v Temperature of vapor

To_a Toth constant a

To_b Toth constant b

To_g Toth constant g

v_v Velocity of vapor

W_{sor} Volume ratio of micro-pores

w_{sor} Specific volume of micro-pores

dp Characteristic void diameter

CHAPTER I

INTRODUCTION

Background

This thesis is a partial summary of work accomplished in an Atmospheric Water Harvesting Computational Research Group AWH CRG under the direction of Dr. Sungwoo Yang at the University of Tennessee at Chattanooga. The primary research aim was to guide development of a device that will adsorb atmospheric water vapor onto an adsorbent followed by a desorption cycle driven by solar irradiation which passes the desorbed vapor inside a chamber where it can be passively condensed. Such devices require negligible energy input and have been shown to be feasible in relative humidity's characteristic of water scarce regions [1, 2]. AWH performance is dramatically influenced by characteristics not well understood with optimization strategies and relationships at the levels of; material, component, device, and operating conditions, an active area of research.

Atmospheric water adsorption evaporation systems are a DOE publicized emerging technology in photothermal-assisted applications. Deliverable devices resulting from research in this area would be deployed in irrigation reclamation, potable water production at the individual and community level, and desalination technologies.

Adsorption is a phenomenon by which an adsorbate in the form of gas or fluid forms films on the surface of a solid adsorbent. Adsorption is divided into chemisorption and

physisorption. Chemisorption describes surface covalent bonding between an adsorbent and adsorbate. Physisorption is the result of electrical structures and attractions inherent to the adsorption pair. The latter involves easily reversible reactions leaving both materials intact and is the mechanism of study. Physisorption is utilized in an array of engineering applications.

Zeolite 13X is the adsorbent selected for study. Zeolites are a common industrial adsorbent and catalyst categorized as a class of oxides that can be naturally found or synthetically designed with customized bonding sites. The material was named in 1756, from the Greek meaning ”to boil” and ”stone” due to the steam that evolved off the material when heated. Zeolite 13X’s thermally dependent hydrophilicity in ranges that are of standard temperature and pressure allow it to be a vapor magnet with flow direction determined by temperature and volume limitations. Zeolite 13X’s uptake/release abilities are improved by its remarkable surface area. Of principal interest to the CRG is the ability to be assess natural, synthetic, and theoretical Zeolite structures for incorporation in an AWH device. IUPAC has endorsed a three class molecular framework scheme; the Faujasites FAU, Mordenite Framework Inverted for ZSM-5, and Mordenite Zeolite for Mordenite, for classifying over 600 discovered Zeolites and an emerging body of synthetic Zeolites. These attributes of Zeolite 13X make it an ideal candidate for design optimization and computational investigation. Engineering applications of Zeolite adsorption systems are typically unit operations represented as batch or alternating fixed bed processes. These processes are accomplished as either pressure swing adsorption (PSA), temperature swing operation (TSA), cryogenic distillation, or purge techniques by way of inert desorbate flooding. The current study focuses on TSA.

Improving adsorption system performance requires understanding numerous model approximations such as; diffusivities, conductivity's, enthalpy's, point charges, and other material characteristics. Figure 1 categorizes a few of these properties. When a molecule of adsorbate adheres to Zeolite an exothermic reaction occurs. This enthalpy creates non-isothermal relationships across the system and further complicates design optimizations. The combination of heat generation and high heat transfer resistance of Zeolites creates a filling/purge bottleneck. Engineering approaches for improving uptake and purge cycling could include material optimization of porosity's, aspect ratios of adsorbent beds, optimization strategies for metal inclusions for heat exchange, phase change thermal storage materials for mitigating latent heat, novel sorbent/substrate structures for heat exchange, modification to sorbent activities and/or modification to selectivity's. Further difficulties in optimization occur when anomalous nano-scale effects occur.

Statement of Problem

AWH requires further study to improve performance by understanding its working mechanisms and optimizing the light adsorber structure [3]. Adsorbent-adsorbate modeling is accomplished with a myriad of factors and relations, any of which could dramatically alter performance predictions. Adsorption model factor sensitivity is not reported and conflicting claims regarding principal modeling sensitives confuse future computational development. Standard approaches overcome these limitations by deriving back-fitted coefficients from experimental work. This limits development and optimization of adsorption/adsorbate systems.

Objectives

This work seeks to build a model that will predict Zeolite 13X and water vapor adsorption. This work seeks to direct computational work regarding the use of this model as it relates to governing equation selection, numerical implementation, model approximations, factor sensitivities, and void confinement limitation detection strategies. Differing approximation equations will be evaluated with a preference for models that have physical meaning and are directly related to micro-structures and forces.

CHAPTER II

LITERATURE REVIEW AND MODEL SELECTION

Modeling techniques such as thermodynamic models, lumped parameters models, heat and mass transfer models, and molecular dynamics models have been applied to adsorption systems. Yong reviewed thermodynamic, lumped parameter, and heat and mass transfer models [4], providing strong form PDE's, major characteristics of each modeling technique, descriptions of differing adsorption models between 1980 and 2002, and numerical implementations pursued by prior researchers with validation techniques. The four main equations composing a heat and mass transfer problem are an energy balance, a mass conservation, a momentum equation, and a state equation. Yong's survey was for nonspecific adsorbent/adsorbate pairs. Survey's of governing equation implementations for Zeolite 13X-Water Vapor were reviewed in [5] and [6]. Sahoo published a COMSOL FEM of natural gas tank filling characteristics study with well described mesh, governing equation, and output statistics equations [7]. Biphasic adsorbent beds for natural gas storage with topological optimization was reported by Amigo [8] building on work by Sahoo with well defined topological optimization techniques for improving adsorbate uptake.

The REV's take thermodynamic relationships, adsorbent properties, adsorbate properties, pressure fields, and temperature fields and approximate finite element model coefficients. The continuum models are a mathematical expression of the 1st and 2nd laws of Thermodynamics. In general, adsorbent-adsorbate heat and mass transfer behavior is governed by four continuum

equations: conservation of energy, conservation of mass, conservation of momentum, and a state equation. Physical properties and observed adsorption isotherms cause these equations to be non-linear. Assumptions regarding thermal equilibrium and mass transfer kinetic equations shape the governing equations.

Governing Equations

Governing equations were researched that characterize the adsorption system in terms for vapor phase, adsorbed phase, and zeolite parameters. The coupled equations express the system dynamics as pressure and temperature fields solving for adsorbed concentration. Mass concentration of vapor adsorbed is represented by, q as kg adsorbed phase per kg of adsorbent. Q represents, kg adsorbed phase per L adsorbent, with derivation by the relationship $Q = (1-\varepsilon_t)\rho_s q$. Bulk density, ρ_b, describes adsorbent density at bed compaction.

Conservation of Mass

$$\frac{\partial(\varepsilon_t \rho_v + (1-\varepsilon_t)\rho_b + Q)}{\partial t} + \nabla \cdot (\rho_v v_v) = 0 \tag{2.1}$$

The density of the vapor phase is considered ideal allowing determination from molar weight of gas (M), universal gas constant (R), domain temperature field, and domain pressure field from the standard relationship, $\rho_v = \frac{M}{R}\frac{P}{T}$.

Zeolite 13X porosity is approximated at two scales. The macropores, ε_{Ma}, consider FAU channel structures, and the micropores, ε_{mi}, consider intra-particle cavities referenced as "cage sites." The bulk density (ρ_b) and crystal density (ρ_c) are used for these calculations.

The $\rho_b = \rho_c * (1 - \varepsilon_{mi})$ approximation [9] with $\varepsilon_{Ma} = 1 - \varepsilon_{mi}$ provide definition for a total effective porosity calculated from , $\varepsilon_t = \varepsilon_{Ma} + (1 - \varepsilon_{Ma}) * \varepsilon_{mi}$. The total effective porosity (ε_t) describes void to total volume. For Zeolite 13X we approximated a total effective porosity of .688.

$$\frac{\rho_v}{\varepsilon_t}\frac{\partial v_v}{\partial t} + \frac{\rho_v}{\varepsilon_t^2} v_v \cdot \nabla v_v = -\nabla P + \mu_v \nabla^2 v_v - \frac{\mu_v}{K} v_v = 0 \tag{2.2}$$

The Navier-Stokes equation in homogeneous isotropic porous flow is presented in equation (2.2). Neglecting, left hand side unsteady and convective terms yields the Brinkman equation. Assuming negligible viscous effects, ($\mu_v \nabla^2 v_v$), resolves Darcy's law which is used to govern vapor velocity with the reduced terms, $v_v = -\frac{K}{\mu_v}\nabla P$. Various approximations for Permeability (K) are considered in the subsequent sections.

Energy Balance

Local Thermal Equilibrium (LTE Model) Equation is constructed from the vapor mass conservation equation and an energy equation. Non Local Thermal Equilibrium (NLTE Model) are constructed from a vapor mass conservation equation, the gas energy equation, and a solid energy equation. Solmus uses a NLTE model for a silica/ water pair [5]. His equations include fluid-solid specific surface area for spherical particles and an inter-facial heat transfer coefficient

for the spherical particles. For this work the LTE is implemented therefore T_s and T_v are assumed equivalent. Of concern are vaporization's points, wherein the LTE equation will lose validity [6].

A local thermal equilibrium dependent equation utilized for coupled vapor, solid, and adsorbed phases was implemented as follows:

$$\varepsilon_t\left(\frac{Cp_vM}{R}\frac{P}{T}\frac{\partial T}{\partial t}-\frac{\partial P}{\partial t}\right)-\frac{Cp_vM}{R\mu_v}K\frac{P}{T}\nabla P\cdot\nabla T$$

$$+(1-\varepsilon_t)(\rho_s Cp_s\frac{\partial T}{\partial t}) \tag{2.3}$$

$$+Cp_{ads}Q\frac{\partial T}{\partial t}-\nabla\cdot(\lambda_{eff}\nabla T)=|\Delta H|\frac{\partial Q}{\partial t}$$

The energy balance for vapor is presented in eq. (2.3) line 1, with Zeolite energy balance presented in eq. (2.3) line 2, and adsorbed phase energy balance in eq. (2.3) line 3. The source term in eq. (2.3) line 3 represents an exothermic reaction connected to adsorption. Various approximation techniques for effective thermal conductivity, (λ_{eff}), are studied below. Specific heat for vapor, (Cp_v), was fitted as a function of temperature [9]. Specific heat for adsorbed phase (Cp_{ads}) and Zeolite specific heat (Cp_{sor}) are constants requiring experimental determination.

Kinetics

For Zeolite 13X water vapor adsorption kinetics the Linear Driving Force model has wide implementation in literature. In a 2002 review of mathematical investigations of adsorption heat pumps Yong references usage of LDF going back to 1989, and reports it as the dominant kinetics equation for a variety of mathematical implementations [4]. Sircar and Hufton demonstrate LDF

as physically and analytically consistent in a comparison study against Fickian Diffusion and Quadratic Driving Force models at constant pressure and at constant volume [10]. Additional comparison was made against a step model by Vermeulen, and a pressure swing adsorption process Nakao Suzuki in a Y.K. Ryu 2001 study [11].

The Chemical Potential Driving Force Model (CPDF) described below was developed from the irreversible thermodynamic assumptions and is considered the most rigorous formulation for describing inter and intracrystalline adsorbate transport [10].

$$J(r,t) = -B \cdot C(r,t)[\frac{\partial(\mu(r,t)/R_g T)}{\partial r}]_t) \tag{2.4}$$

The Linear Driving Force model described below has a single lumped parametric coefficient, G, that is called the effective LDF mass transfer coefficient.

$$\frac{\partial Q}{\partial t} = G(Q_{eq} - Q) \tag{2.5}$$

The LDF mass transfer coefficient,G, is investigated below. The transfer coefficient is understood to be dependent on vapor loading [10]. The LDF transfer coefficient is the implemented in the current code with several variations considered.

Gas / Solid Isotherm Equations, Q_{eq}

Classic Isotherms have required modifications at pressures exceeding critical pressure. The thermodynamic inconsistency make assumptions regarding localization vs mobility, and interaction effects vs no interaction effects. Classic isotherm equilibrium equations required

modification at pressures over critical pressures to account for a neglected accounting of differences between gas phase density and adsorbed phase densities. Toth noted that the infinitely great change in relative free energy as surface coverage varies from 0 to 1 [12]. Figure 2.1 compares our utilized isotherms with critical notation for the point of capillary condensation which occurs above 0.3 relative pressure. Capillary condensation causes breakdown in predictive in BET and Langmuir based.

Table 2.1 Equilibrium Isotherms: $C = exp\frac{H_i - H_1}{RT}$, Relative Pressure $= \frac{P_{eq}}{P_o}$

Model	Citation	Structure
mBET	Bashiri[13]	$\frac{V}{Vm}[\frac{mol}{kg}] = \frac{(C\frac{P_{eq}}{P_{sat}})^{BET\alpha}}{(1-\frac{P_{eq}}{P_{sat}})(1-\frac{P_{eq}}{P_{sat}}+(C\frac{P_{eq}}{P_{sat}})^{BET\alpha})}$
DA	Ambrozek[14]	$exp\left\{-\left[\frac{RT}{E_O}ln(\frac{P_{sat}}{P_{eq}}\right]^{n_s}\right\}$
Toth	Narayanan[9]	$n[\frac{mol}{kg}] = \frac{ap_{eq}}{(1+(bp_{eq})^g)^{\frac{1}{g}}}$

Modified Brunauer-Emmett-Teller (BET)

The BET model is widely used to describe multi-layer adsorption among Type II-Isotherms. Saturation pressure (P_0) and a fitting parameter calculated from Adsorption Enthalpies (C_{BET}) dominate the approximation. A modified BET could be utilized in future implementations which a heterogeneity (BET_α) parameter is incorporated [13].

Young Ryu reports a 1998 finding from Do that for relative pressure above 0.3 capillary condensation occurs and a multilayer isotherm such as BET would would fail. Ryu notes that capillary condensation pressure strongly depends on system temperature and saturated pressure [11].

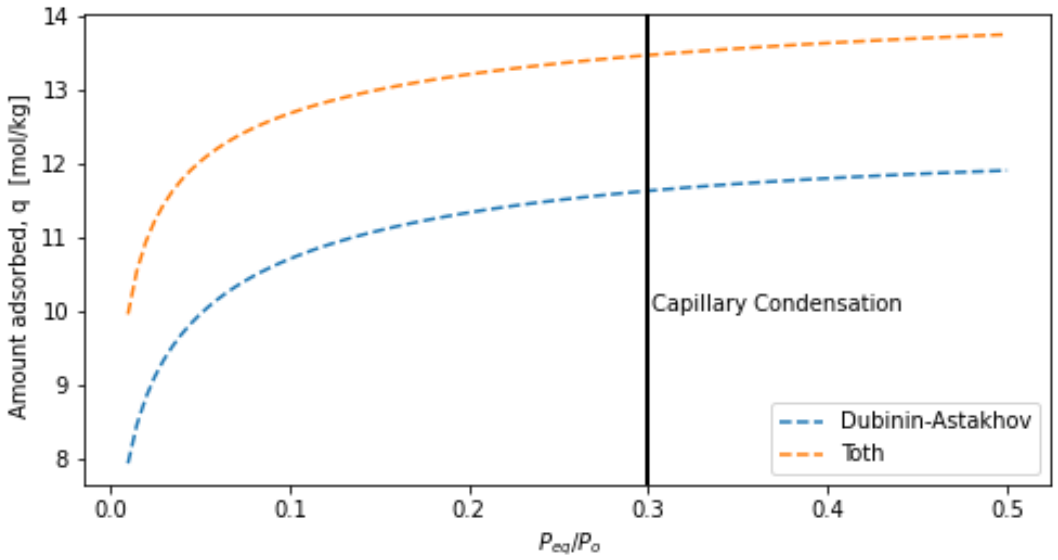

Figure 2.1 Isotherms

Permeability

Kozeny-Carman equations are used to approximate pressure drop as vapor flows through the sorbent. The equation assumes laminar flow and does not hold for Reynold numbers exceeding 1.0.

Kozeny extrapolated Hagen-Poiseuille flow equations and Darcy's law with the concept of tortuosity, a ratio of actual length of flow path in porous media to length without media, to produce approximations for predicting capillary flow. Carman and Kozeny developed approximations for flow through a packed bed of spheres. The reworked equations created the Kozeny constant which considers; tortuosity, particle shape, and their connections. A literature study of 23 determinations [15] for the Kozeny constant describes wide ranging conclusions with none considering micro-structural parameters. We consider three Kozeny-Carman equations previously used in literature.

Both the Kozeny constant and tortuosity averaging introduce significant opportunity for model miss-characterization.

Table 2.2 Permeability: with computed values for the simulation

Model	Structure	Value $[m^2]$
Kozeny-Carman Effective Porosity, [7], [9]	$K = \frac{2r_s^2\varepsilon_M^3}{75(1-\varepsilon_M)^2}$	2.189e-20
Kozeny-Carman, pore tortuosity [7]	$K = \frac{2\phi_s^2\varepsilon_M^3}{72\tau(1-\varepsilon_M)^2}$	2.280e-20
Kozeny-Carman, Kozeny constant	$K = \frac{\phi_s^2\varepsilon_M^3}{36k_k(1-\varepsilon_M)^2}$	1.900e-20

Diffusivity

The linear driving force model lumped parameter represented above as G in equation (2.5) considers external film resistance, macro-pore resistance, and micro-pore resistance. Ryu cites a Nakao Suzuki finding that at low adsorbed vapor concentration the G coefficient originally presented by Gluceckauf and Coates, underestimates the rate of uptake [11] .

An implementation of the generalized Maxwell-Stefan Model by [16] provided a multi-component mass transfer of adsorbed species across zeolite membranes. This model allows for distinction between surface diffusivity's and cross-species interactions. This cross species interactions is a potential area for AWH development. Models that allow for specifying multiple species of temperature dependent adsorbate selectivity's, and temperature dependent surface diffusivity's allow for another design element in atmospheric water harvesting. Purge gases or

gases selected by the zeolite itself could further allow engineering for desired effective thermal conductivity's and effective diffusivity's.

Table 2.3 Linear Driving Force Coefficients for Mass Transfer

Model	Structure
Vasiliev [17]	$\frac{D_M}{\mu}\frac{M\varepsilon_t}{\rho_s R_g T}\frac{1}{\partial}$
Ambrozek [18]	$\frac{15D_{s0}}{r^2}exp(\frac{-E_a}{Rt})$
Narayanan [9]	$\varepsilon^{\frac{3}{2}}\frac{dp}{3}\sqrt{\frac{8Rt}{\pi M}}$
Knudsen Diffusivity [9]	$D_{s0}e^{\frac{-E_a}{RT_0(1-\frac{T}{T_0})}}$

In addition to the determination of conversion, yield, and selectivity, calculation of the activation energy and the determination of the Thiele modulus and the effectiveness factor are good indicators of the presence or absence of diffusion limitations in hierarchical zeolite [19].

Effective Thermal Conductivity

The modeling of heat transport through porous media is a widely researched area covering many disciplines and industries with mathematical descriptions for granular materials, dispersed spheres, fibrous composites, and packed beds available for review. Several factors related to thermal conductivity have limited the development of micro-porous adsorbent systems. Heat transfer is currently the rate limiting step and major leaps forward in the deployment of these

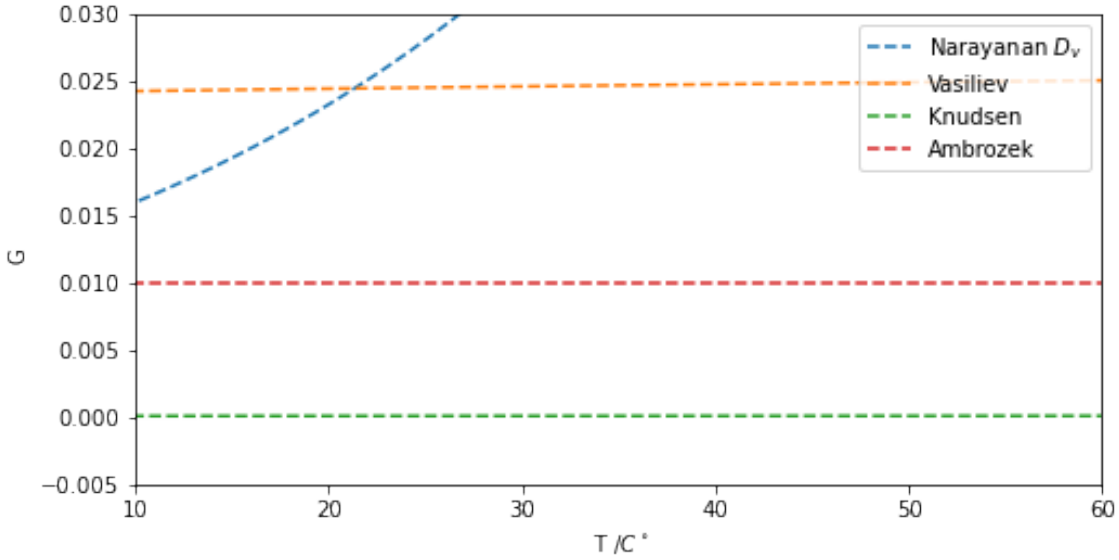

Figure 2.2 Diffusivity comparisons

materials will be in this area. Low pressure adsorbent designs are blinded by poorly understood Knudsen effects limiting a proper characterization of radiative and conductive heat transfers. Standard solutions to optimize heat transfer such as; plate-fin heat exchangers, embedded composites, and surface coatings require accurate effective thermal conductivity calculation before optimized designs can be presented.

Broadly thermal conductivity models fall into two mathematical expressions, Fourier's law models solving a Laplace Equation and Ohm's law solving a one-dimensional heat flow. Most models consider solid and fluid phases only with only a few theoretical models that predict the effective thermal conductivity's of multi-phase materials. Some modelers combine theories and create weighting functions to calculate the effective thermal conductivity [20].

Table 2.4 Thermal Conductivity

Model	Structure
Effective Thermal Conductivity [7]	$\lambda_{eff} = \varepsilon_t \lambda_g + (1-\varepsilon_t)\lambda_s$
Maxwell-Eucken [8]	$k_f(\varepsilon_t) = k_s \frac{k_g+2k_s+2\varepsilon_t(k_g-k_s)}{k_g+2k_s-\varepsilon_t(k_g-k_s)}$
Modified Zehnder-Schlunder [2]	$\frac{k_{eq}}{k_g} = (1-\sqrt{1-\varepsilon}) + \frac{1-\sqrt{\varepsilon}}{\gamma}$ $+(\sqrt{1-\varepsilon}+\sqrt{\varepsilon}-1)\cdot\left[\frac{b\cdot(1-\gamma}{(1-\gamma\cdot b)^2} ln\frac{1}{\gamma\cdot b} - \frac{b-1}{1-\gamma\cdot b}\right]$ $b = \left(\frac{1-\varepsilon}{\varepsilon}\right)^m, m = 0.9676, \gamma = \frac{k_g}{k_z}$

A multiphase effective thermal conductivity model that considers Poiseuille flow ($Kn < 0.01$) effects, Knudsen flow effects ($.01 < Kn < .05$), and Molecular flow effects ($Kn > .5$) is needed.

Effective thermal conductivity calculations built from back-fitted data or general material properties for solid, liquid, and gas phases are typically used. These types of models fail to consider adsorbed phase conductivity under novel pressure and temperatures with capillary condensation, and asymmetric void filling near high heat transfer material in addition to other anomalous phenomenon that might be occurring.

ISOSTERIC HEAT OF ADSORPTION

The heat of adsorption is the amount of energy released when water vapor is adsorbed to a surface. This property is a unique to sorbent/sorbate interactions. The property has been utilized to; characterize surface heterogeneity or homogeneity, film formation, and the heat of condensation [21]. The property is determined by a variety of techniques, two are tested both derived from the Clapeyron equations. There are molecular dynamic simulations that produce estimates for the Isosteric Heat of Adsorption. The Clausius-Clapeyron equations with assumptions for ideal gas

conditions and assumption for an excess of bulk vapor phase to adsorbed vapor phase reduces to the Van't Hoff equation. The Van't Hoff equation can be computed directly from FEM shape functions using such a calculation.

Table 2.5 Isosteric Heat of Adsorption

Model	Structure
Vant Hoff (Backfitted [9]	$\Delta H = C_1 + C_2 * \frac{Q_{eq}}{M}$
Vant Hoff Relative Pressure [22]	$\Delta H = H_{vap} + RTln(\frac{P_{sat}}{P_{eq}}) + \frac{\alpha RT}{n\beta E_O}(Tln\frac{P_s}{P_{eq}})^{1-n}$, $\alpha = \frac{1}{T^2}\frac{\partial ln(\frac{\rho_{ads,max}}{\rho_{ads,actual}})}{\partial \frac{1}{T}}$

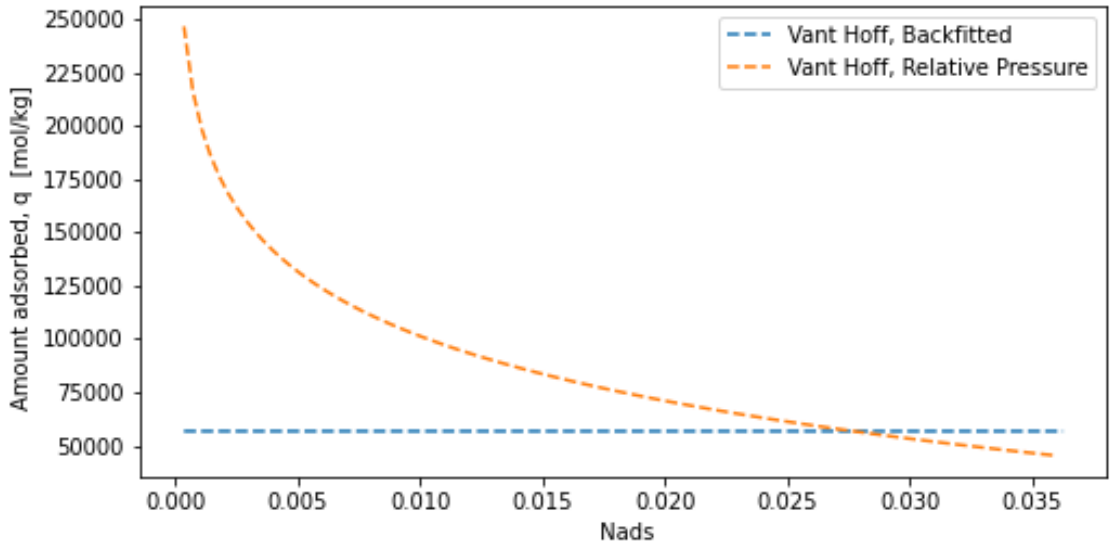

Figure 2.3 Isosteric Heat of Adsorption: The above graphic was not generated from FEM results. They were calculated from error checking test scripts. The use of density concentrations will have a dramatic effect on FEM inputs. This graphic helps to illustrate the unrealistic nature of back fitted input methods

Another technique for estimating Isosteric Heat of Adsorption from the thermodynamic relationships utilizes entropy balances. This technique was not implemented for this study.

Saturation Adsorbed Density

The temperature dependence of adsorbate density is a critical characteristic. The adsorbate density models in Table 2.6 can be understood using the terms, T_c critical temperature, α represents a well known value with the thermal expansion coefficient determined by experimentally fitting the coefficient to the slope of ρ-T diagram. For this effort we used reference α.

Table 2.6 Adsorbate density models

Antoine Eq. [9]	$\rho_{ads} = BC^{-(1-T/T_c)^m}$
Mugele [23]	$\rho_{ads} = \frac{\rho_{20^\circ C}}{1+\alpha_{ads,20^\circ C}(T-293.15K)}$
Hauer [23]	$\rho_{ads} = \rho_{10^\circ}[1-3.781\cdot10^{-4}(T-283.15K)]$
Dubinin [23]	$\rho_{adg} = \frac{\rho_c}{exp(\alpha(T-T_c))}$

Simulation Robustness

Dimensionless parameters to categories adsorption systems are identified and discussed. These parameters are intended to describe the ability of the numerical method to provide a solution within control parameters and known limitations for implemented equations. The Knudsen number, Reynolds number, Forcheimer number, and Diffusional Time Scales are considered.

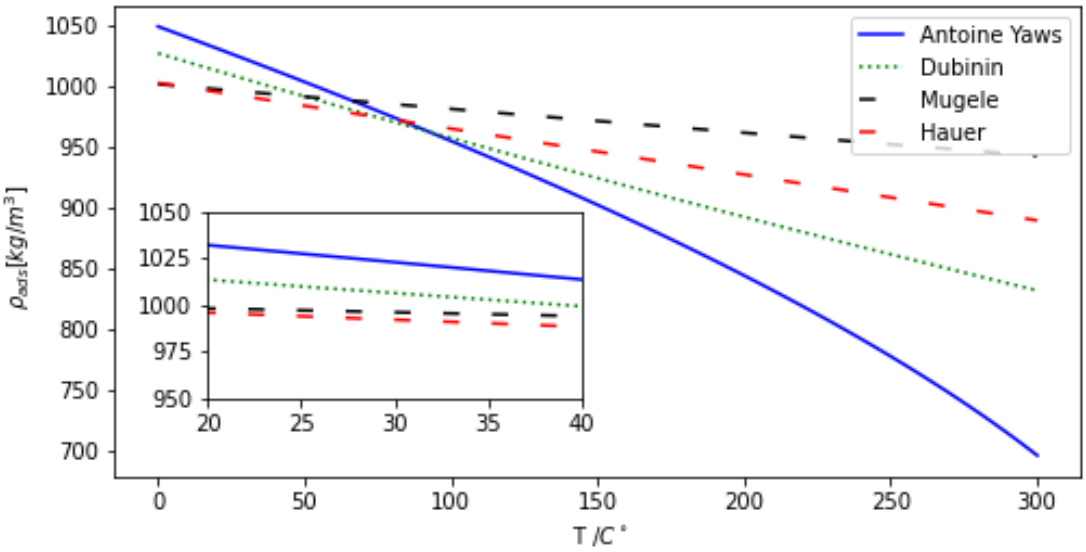

Figure 2.4 Adsorbate density equations with inset representing anticipated operational ranges

Non-Darcy Effects

The Reynolds number is used under the assumption that Non-Darcy effects in porous media are analogues to turbulence. Research in this area is needed. Transition regions between .1 to 1000 need further delimitation. The temperature dependent density of vapor, temperature and concentration dependent viscosity, vapor velocity, and characteristic particle diameter express this Reynolds number

$$Re = \frac{\rho_v \phi_{sor} v_v}{\mu} \tag{2.6}$$

A Forcheimer number of .11 is a Darcy law validity check in porous media. A F_O of .11 approximates 10% of forces result from Non-Darcy effects.

$$[8]F_O = \frac{\rho_g K \beta v_g}{\mu} \tag{2.7}$$

The density of vapor, permeability, β, particle diameter, velocity, and viscosity are required. The β is found by measuring pressure drop in adsorbent at different flow rates. This also requires further validation in literature.

Diffusion Time Scales

$$\gamma = \frac{D_\mu l^2}{\sigma D_v r_c^2} \tag{2.8}$$

When γ is approximately 1 or greater vapor transport in inter-crystalline pores is expected to be much slower. Macro-pore diffusion is then the rate limiting step. However, when $\gamma < 1$ intracrystalline diffusion is much slower and micro-pore diffusion sets the vapor uptake limits. σ defines relative vapor storage capacity of macro and micro-pores. l represents the characteristics length, and r_c represents crystal radius [9].

The adsorption speed appears to be limited by adsorbed mass and resistance to heat transfer [24]. In general models neglecting Non-Darcy effects have good experiment results.

The Navier-Stokes equations assume that the free path of a particle is smaller than the length of the system. For adsorption systems gas molecule-surface interactions can generate non-equilibrium effects. The physics of this is believed to be molecules colliding with the wall

more frequently than with other molecules. This effect becomes know as a Knudsen layer. Few researchers have included non-equilibrium effects in a Navier-Stokes framework [25].

CHAPTER III

METHODOLOGY

Several assumptions are made in this REV scheme; that the porous medium is homogeneous and isotropic, that the porous particles are incompressible, that compression work and viscous dissipation are negligible, that inter particle radiation is linearized and included in the heat exchange solid-gas coefficient and the solid thermal conductivity, that the dispersion's terms and tortuousity terms can be modeled as diffusive fluxes, and that the water vapor phase is ideal from thermodynamic view points. Darcy's law is used to calculate velocity as a pressure gradient. The energy equation assumes local thermal equilibrium. The Lagergren model is used to describe kinetics as rated limited by adsorption and not film resistances.

Boundary Conditions and Domain Assignments

The domain Ω and boundaries Γ of computational study are outlined in Figure 3.1. The model presented is for conditions of studying the adsorption phase. Desorption temperature and pressure conditions will require alternative definition determined by vapor collection and condensing designs.

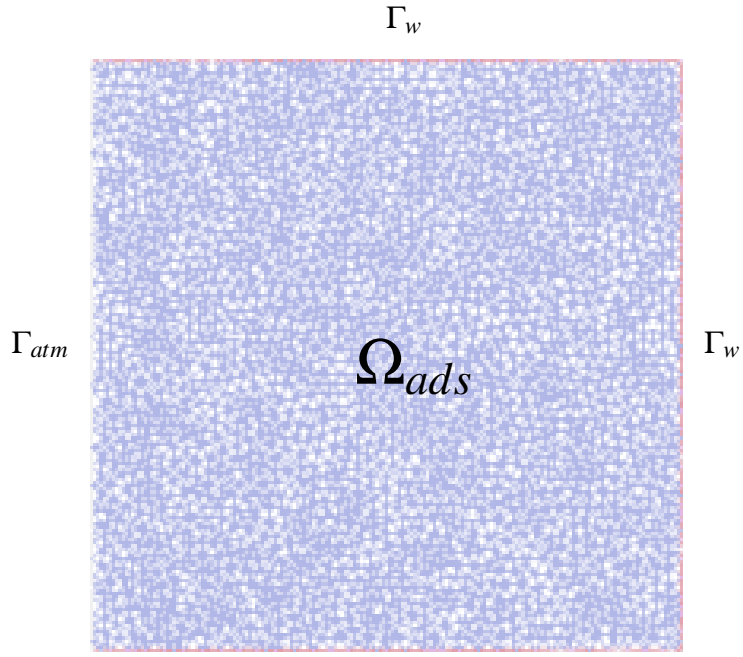

Figure 3.1 2D geometry with mesh refinement around, walls, vapor intake, and heat sink. Domains and boundaries are identified by specifying equations and alternative material characteristics

The atmospherically exposed sorbent face, Γ_{atm}, is expressed for heat flux by the following Robin boundary condition:

$$-k_f \frac{\partial T}{\partial n} = \frac{M_g C p_g K}{R \mu_g} \frac{P}{T} \nabla P \cdot n (T - T_{atm}) \tag{3.1}$$

Due to the assumption of local thermal equilibrium the inlet temperature is assumed equal to the atmospheric temperature during periods of adsorption and is considered as a Dirichlet (T = T_∞).

Walled portions, Γ_w, of the harvester are modeled as convective heat flux boundaries expressed as a Robin boundary conditions:

$$-k_f \frac{\partial T}{\partial n} = h_W (T - T_{atm}) \tag{3.2}$$

A Robin boundary condition governs the mass flux for determination of fixed mass flows.

$$\rho_v v_v \cdot n = \dot{q} \tag{3.3}$$

During the adsorption cycle the mass flow boundary represents a fixed partial pressure of water vapor supplied by an atmospheric infinite reservoir. Desorption off-gassing is not drawn from infinite reservoir and fixed values of partial pressure of water vapor should not be assumed. Current specifications have partial vapor pressures desorbing back to atmospheric vapor pressures. Alternative pressures can be set for future work exploring vapor collection designs.

Shape Functions, Function Spaces, and Solver Parameters

A mixed element code design was utilized in FEniCS with shape function assignments for temperature and pressure as Lagrange polynomials with degree 1. Continuous Galerkin basis functions were defined for specific heat, pressure, temperature, and entropy. A density function space was specified on the mesh as a discontinuous Galerkin basis function. The density function assigned values from projections of kinetic and equilibrium equations.

The applied variational function forms are nonlinear. The numerical implementation approximates the solution field and linearizes a perturbation derivative by assuming sufficiently small changes in a forward Euler calculation. The perturbation derivative is calculated over the mixed element space as a Gateaux derivative in the direction of our the trial space resulting in a Jacobian that is automatically calculated at each timestep.

The PETSc KSP GMRES packages solve the Jacobian calculated from the set of discrete non-linear equations. The GMRES package was set with maximum tolerance of $1e-5$ and maximum iterations of 25. The KSP package allows monitoring of preconditioned residual norm and true residual norms which assists in the determination of adequate spatial and temporal time stepping. The Jacobian form was specified which allows the use of a nonlinear solver using Newton's method.

Model Verification

Spatial Stepping Determination

A spatial convergence study of 9 trials was conducted. An unstructured mesh was generated with an increasing number of spatial steps for each trial. The mesh was considered spatially converged when an increase in the mesh spatial resolution no longer altered the models determination of Mass of Vapor Adsorbed, m_{ads}. Mass of Vapor Adsorbed was assembled from the nodal elements for density of adsorbed vapor, ρ_{ads} and an axis factor, V_b.

$$\text{Mass of Adsorbed Vapor (kg)}, m_{ads} = (1-\varepsilon_t)\rho_{ads}V_b \tag{3.4}$$

Temporal Stepping Determination

A temporal convergence study of 9 trials was conducted. Total simulation time was held constant while time stepping was increasingly resolved. The time stepping scheme was considered converged when the increased resolution no longer impacted the predicted amount of Mass of Vapor Adsorbed.

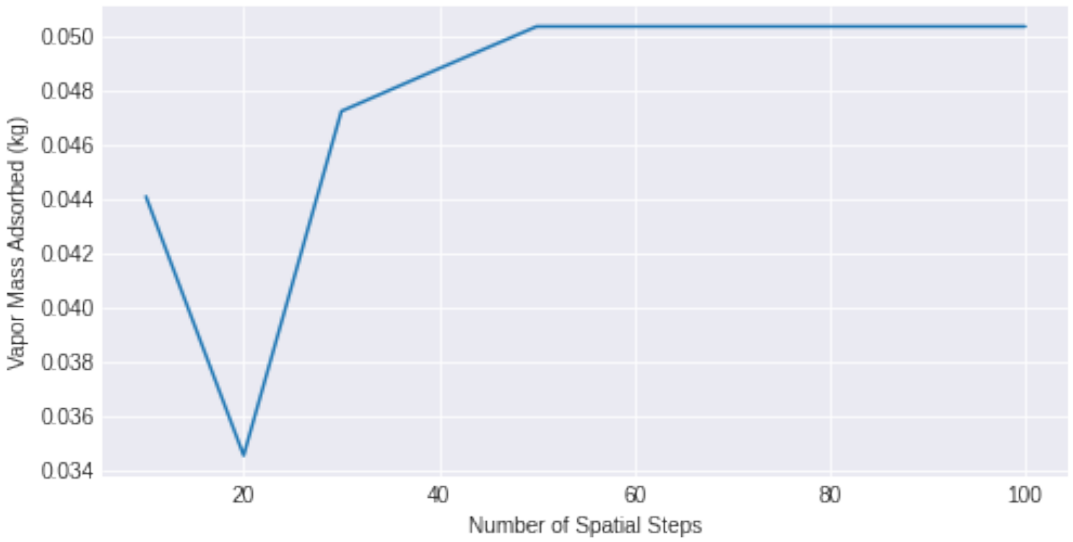

Figure 3.2 Spatial Convergence Study: The mesh adequately resolved at nx = 50. nx = 60 was used for subsequent investigation

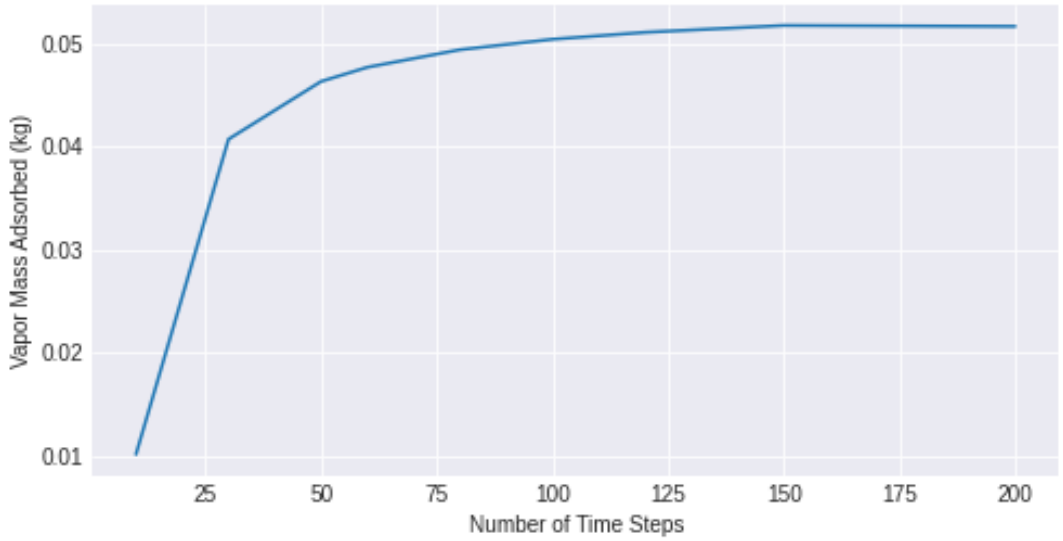

Figure 3.3 Temporal Convergence Study: The time stepping adequately resolved at nt = 125. nt = 150 was used for subsequent investigation

Validation Study

The simulation solved across a range of partial vapor pressures while holding thermal equilibrium at 25 ° C. The results of those simulations are presented in Figure 3.4 which is an Isotherm Loading plot. The simulations were compared against Yu Wang and M. Douglas LeVan published results for determining the Adsorption Equilibria of Pure Water Vapor on Zeolite 13X by way of the volumetric method [26].

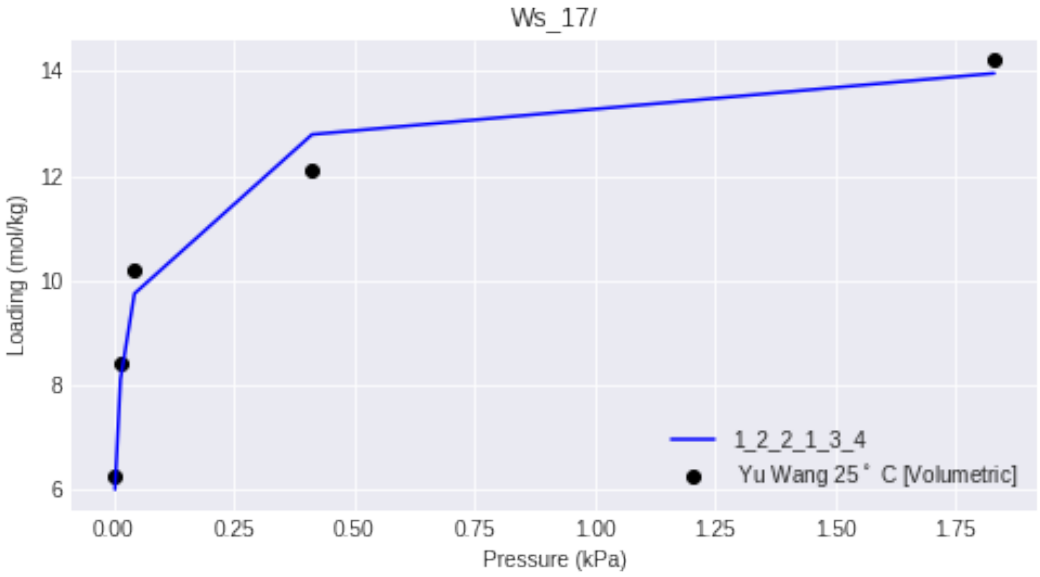

Figure 3.4 Validation Study Results: Isotherm Loadings

Figure 3.4 plots the volumetrically determined Adsorption Equilibrium are plotted in black with simulation results in blue. The model was specified with the Dubinin-Astakhov for adsorption density equilibrium, Vant Hoff fitting for the enthalpy of adsorption, Vasiliev method for the mass transfer coefficient, Kozeny-Carman approximation with no constants for permeability, Modified

Zehnder-Schlunder for effective thermal conductivity, and Antoine fitting for the local adsorbed gas density.

CHAPTER IV

RESULTS

Factor Screening

The complexity of the numerical solver obfuscates the models sensitivity to its input factors. A factor screening was conducted to investigate which factors have a significant impact on a performance measure. Eight model factors were selected as control variables. These factors are the material characteristics that get specified as constants in the simulations. The factors studied include bulk density (ρ_b), thermal conductivity of adsorbent λ_{sor}, micropore dispersion (n_s), specific heat capacity of adsorbent (Cp_{sor}), activation energy of adsorption (E_a), energy of adsorption (βE_O), mean value of thermal expansion (α), and inter-crystalline gas diffusivity(D_{sO}). The response variable is the adsorbed vapor density from a mixed element Discontinuous Galerkin function space assembled by the simulation every ten timesteps.

The simulation constructed for factor screening utilized the same approximation techniques as the validation study. The adsorption density equilibrium was determined by the Dubinin-Astakhov. The enthalpy of adsorption was found by Vant Hoff fitting. The mass transfer coefficient was found by the Vasiliev method. Permeability determined by Kozeny-Carman approximation with no constants. The effective thermal conductivity was found by modified Zehnder-Schlunder. Modeling noise factors could emerge from such approximation techniques. Each timestep a Jacobian is calculated and Newton Methods are used for converging to solution. If noise factors

enter due to approximations they would be expected to be normally distributed and randomize. Non-randomizing noise factors would most likely create intolerance's that prevent convergence.

The factor screening was performed using a 2^k full factorial design. This experimental design utilizes analysis of variance techniques comparing 256 simulated trials against a variety of factorial specifications. Each factor was replaced with high and low value. A design matrix was constructed which prescribes the necessary placement of high and low factorial values for each trial. The factor screening results quantify the difference in adsorption uptake between the high and low factor values. The full factorial design can determine interaction effects for all possible combinations. Two studies were conducted; a moderately spaced study and an aggressively spaced.

Table 4.1 Moderate spacing values represent a 10% differential and the aggressive spacing represent a 20% differential. $'-'$ represents significance effects that had a p-value higher than .05

Factor Significance Effects on Uptake $[kg/m^3]$		
Factor	Moderate Spacing	Aggressive Spacing
D_{sO}	-0.2127	-0.41442
n_s	.2112	0.47182
βE_O	.0961	0.22231
E_a	.04306	0.08196
E_a and D_{sO}	.00625	.026341
ρ_b	-	-
λ_{sor}	-	-
Cp_{sor}	-	-
α	-	-

The significance effects are described in Table 4.1. These results show this modeling to be most sensitive to inter-crystalline gas diffusivity and micro-pore dispersion. The energy of adsorption and the activation energy of adsorption have a statistically significant result at moderate

spacing with the energy of adsorption become a more significant value at its aggressive spacing. It was surprising to not see effective thermoconductivity produce statistically significant results.

CHAPTER V

CONCLUSION

A Finite Element Model for use in the development of Zeolite 13X adsorption system was developed. It was found that a large and diverse body of work exists for adsorption modeling with little consensus on which modeling techniques should be considered standard. Computational research groups working in this area should repeatedly make assessment of factor inputs and the mathematical approximations describing physical behavior. To understand the differences in some of these techniques a model was developed that can quickly execute six different libraries of system behavior approximations. Three adsorption density equilibrium equations were constructed; the Dubinin-Astakhov, the Toth, and a Dubinin-Radushkevich. Three heat of adsorption options were created; a constant, Narayanan fitting equation, and Cortes relative pressure approximations. Four mass transfer coefficients were developed; a constant, the Vasilev, Knudsen, and an effective intercrystalline diffusivity. The permeability library had three implementations; Kozeny-Carman with tortusoity, Kozeny-Carman by effective porosity, and Kozeny-Carman with kozeny constant. The Effective thermal conductivity library included; effective thermal conductivity, Maxwell-Eucken, Modified Zehnder-Schlunder, and a secondary implementation of the Zehnder-Schlunder. A library for implementing local gas adsorption included; Mugele, Hauer, Osawa, and Antoine equations. Once the model was verified and validated it was analyzed for factor sensitivity. It was

expected that factors related to heat management would steer water uptake. Instead it was found that micro-dispersion factors and diffusivity interactions are driving performance.

Based on the findings of this work a molecular dynamic simulation capable of approximating intra-crystalline gas diffusivity is being constructed. In addition a shape fitting algorithm written for placing heat sink metal in the adsorbent is being constructed to describe the ideal placement of vapor transfer channels. The shape optimizing multi-scale model being constructed should be able to replace time consuming and expensively obtained experimental values which are required to describe novel material and system designs for adsorption based atmospheric water extraction using nano-porous materials.

REFERENCES

[1] Chao Zhang, Hong Qing Liang, Zhi Kang Xu, and Zuankai Wang. Harnessing Solar-Driven Photothermal Effect toward the Water–Energy Nexus. *Advanced Science*, 6(18), 2019. 1

[2] Hyunho Kim, Sameer R. Rao, Alina LaPotin, Seockheon Lee, and Evelyn N. Wang. Thermodynamic analysis and optimization of adsorption-based atmospheric water harvesting. *International Journal of Heat and Mass Transfer*, 161:1–7, 2020. 1, 15

[3] Zhihui Chen, Shiyu Song, Benchi Ma, Yueqi Li, Yu Shao, Jinwen Shi, Maochang Liu, Hui Jin, and Dengwei Jing. Recent progress on sorption/desorption-based atmospheric water harvesting powered by solar energy. *Solar Energy Materials and Solar Cells*, 230(March):111233, 2021. 3

[4] Li Yong and K Sumathy. Review of mathematical investigation on the closed adsorption heat pump and cooling systems. 6:305–337, 2002. 5, 8

[5] Ismail Solmuş, D. Andrew, Cemil Yamali, and Derek Baker. A two-energy equation model for dynamic heat and mass transfer in an adsorbent bed using silica gel/water pair. *International Journal of Heat and Mass Transfer*, 55(19-20):5275–5288, 2012. 5, 7

[6] A. Mhimid. Theoretical study of heat and mass transfer in a zeolite bed during water desorption: validity of local thermal equilibrium assumption. *International Journal of Heat and Mass Transfer*, 41(19):2967–2977, 1998. 5, 8

[7] Pradeepta K. Sahoo, Mathew John, Bharat L. Newalkar, N. V. Choudhary, and K. G. Ayappa. Filling characteristics for an activated carbon based adsorbed natural gas storage system. *Industrial and Engineering Chemistry Research*, 50(23):13000–13011, 2011. 5, 12, 15

[8] R C R Amigo. Design of Adsorption Systems by using Topology Optimisation Design of Adsorption Systems by using Topology Optimisation. page 136, 2018. 5, 15, 19

[9] Shankar Narayanan, Sungwoo Yang, Hyunho Kim, and Evelyn N. Wang. Optimization of adsorption processes for climate control and thermal energy storage. *International Journal of Heat and Mass Transfer*, 77:288–300, 2014. 7, 8, 10, 12, 13, 16, 17, 19

[10] S. Sircar and J. R. Hufton. Why does the linear driving force model for adsorption kinetics work? *Adsorption*, 6(2):137–147, 2000. 9

[11] Young Ki Ryu, Seung Ju Lee, Jong Wha Kim, and Chang-Ha Leef. Adsorption equilibrium and kinetics of H2O on zeolite 13x. *Korean Journal of Chemical Engineering*, 18(4):525–530, 2001. 9, 10, 12

[12] Jozsef Toth. Modifications in classic relationships corresponding to gas/solid physical adsorption. *Journal of Colloid and Interface Science*, 191(2):449–455, 1997. 10

[13] Hadis Bashiri and Samaneh Orouji. A new isotherm for multilayer gas adsorption on heterogeneous solid surfaces. *Theoretical Chemistry Accounts*, 134(1):1–7, 2015. 10

[14] B. Ambrozek, W Zwaryez-Makles, and W Szaflik. Equilibrium and Heat of Adsorption for Selected Adsorbent-Adsorbate Pairs Used in Adsorption Heat Pumps. *Polska Energetyka Słoneczna*, pages 5–11, 2012. 10

[15] Turkuler Ozgumus, Moghtada Mobedi, and Unver Ozkol. Determination of kozeny constant based on porosity and pore to throat size ratio in porous medium with rectangular rods. *Engineering Applications of Computational Fluid Mechanics*, 8(2):308–318, 2014. 11

[16] Saeed Shirazian and Seyed Nezameddin Ashrafizadeh. Investigations on permeation of water vapor through synthesized nanoporous zeolite membranes; A mass transfer model. *RSC Advances*, 5(39):30719–30726, 2015. 12

[17] Barbara Mette, Henner Kerskes, Harald Drück, and Hans Müller-Steinhagen. Experimental and numerical investigations on the water vapor adsorption isotherms and kinetics of binderless zeolite 13X. *International Journal of Heat and Mass Transfer*, 71:555–561, 2014. 13

[18] L. L. Vasiliev, L. E. Kanonchik, and V. A. Babenko. Thermal management of the adsorption-based vessel for hydrogeneous gas storage. *Journal of Engineering Physics and Thermophysics*, 85(5):987–996, 2012. 13

[19] Martin Hartmann, Matthias Thommes, and Wilhelm Schwieger. Hierarchically-Ordered Zeolites: A Critical Assessment. *Advanced Materials Interfaces*, 8(4), 2021. 13

[20] K. C. Chan, Christopher Y.H. Chao, G. N. Sze-To, and K. S. Hui. Performance predictions for a new zeolite 13X/CaCl 2 composite adsorbent for adsorption cooling systems. *International Journal of Heat and Mass Transfer*, 55(11-12):3214–3224, 2012. 14

[21] Richard T. Cimino, Piotr Kowalczyk, Peter I. Ravikovitch, and Alexander V. Neimark. Determination of Isosteric Heat of Adsorption by Quenched Solid Density Functional Theory. *Langmuir*, 33(8):1769–1779, 2017. 15

[22] F. B. Cortés, F. Chejne, F. Carrasco-Marín, C. Moreno-Castilla, and A. F. Pérez-Cadenas. Water adsorption on zeolite 13X: Comparison of the two methods based on mass spectrometry and thermogravimetry. *Adsorption*, 16(3):141–146, 2010. 16

[23] Thomas Nagel, Steffen Beckert, Norbert Böttcher, Roger Gläser, and Olaf Kolditz. The Impact of Adsorbate Density Models on the Simulation of Water Sorption on Nanoporous Materials for Heat Storage. *Energy Procedia*, 75:2106–2112, 2015. 17

[24] Mhiri Foued. Kinetic study for the adsorption of vapour water adsorption on zeolite 13× and silica gel. *2012 1st International Conference on Renewable Energies and Vehicular Technology, REVET 2012*, pages 116–124, 2012. 19

[25] Apurva Bhagat, Harshal Gijare, and Nishanth Dongari. Modeling of knudsen layer effects in the micro-scale backward-facing step in the slip flow regime. *Micromachines*, 10(2):1–15, 2019. 20

[26] Yu Wang and M. Douglas LeVan. Adsorption equilibrium of carbon dioxide and water vapor on zeolites 5a and 13X and silica gel: Pure components. *Journal of Chemical and Engineering Data*, 54(10):2839–2844, 2009. 26

VITA

Evan Gildernew got his undergraduate degree from the University of Tennessee at Chattanooga before deciding to stay on as a graduate student. He has been the recipient of a Research Assitantship in Applied Mathematics under Eleni Panagiotou studying the visco-elsastic reponse of long chain polymers. He was also awarded a Research Assistantship in Chemical Engineering under Sungwoo Yang studying atmospheric water harvesting.